# Green synthesis, structural characterization and application of cadmium sulfide nanocrystals with fluorescent dyes for solar enhancement

**Yashvant Rao[1], Gajendra Kumar Inwati[1], Man Singh[1,2]***

[1]*Centre for Nanosciences, Central university of Gujarat, Gandhinagar 382030, India*
[2]*School of Chemical Sciences, Central university of Gujarat, Gandhinagar 382030, India*

*Corresponding author, Tel: (+91) 7923260340; Fax: (+91) 7923260076; E-mail: mansingh50@hotmail.com

**Received: 14 March 2016, Revised: 12 November 2016 and Accepted: 15 December 2016**

DOI: 10.5185/amp.2017/404
www.vbripress.com/amp

## Abstract

Cadmium sulphide nanocrystals (CdS NCs) of ≈ 7.0 nm have been synthesized and structurally characterized with X-Ray Diffraction (XRD), High Resolution Transmission Electron Microscope (HR-TEM) and topographical 3D image by Atomic Force Microscopy (AFM). The binding and kinetic energies of 5$^{th}$ electron of 3d orbital (inner $3d_{5/2}$) and 3$^{rd}$ (outer $3d_{3/2}$) of Cd were 405.93 and 412.67 eV as well as 1074 and 1080.76 eV respectively determined with XPS. The CdS at 298.15 K, when dispersed in water, methanol and ethanol with 100 µM each of rhodamine B (RB), sulphorhodamine B (SRB) and carboxyfluorescein (CF) the fluorescent dyes (FD) separately has enhanced UV-Vis absorbance by 45, 30 and 25% respectively in order of (RB-CdS) > (SRB-CdS) > (CF-CdS) within 200 to 320 nm as compared to without CdS. Probably the CdS has functionalized the functional groups of the dyes that could have induced the π-conjugated bonds to detain higher UV-Vis abs. especially one -COOH, four -$CH_2CH_3$, two -$SO_3$, four -$CH_2CH_3$ and two –COOH, one >C= with one hydroxyl group respectively. Thus, the CdS-Dye-UV-Vis model could be proposed as new finding of our studies. 

**Keywords:** CdS NCs, crystal structure, photoelectrons, fluorescent dyes.

## Introduction

The emerging area of research in nanoscience and nanotechnology, have been drawn a lot of attraction and attention on account of their enormous applications in LCD, solar cells, quantum dots, nano-biotechnology and others. Here we synthesized the CdS NCs in heterogeneous medium and have been characterized including their optical density with RB, SRB and CF. Now the CdS NCs is a subject of huge discussion due to their nonlinear properties, quantum size effects and other fundamental physicochemical and biological **[1, 2]** properties of quantum dots (QDs) of CdS can be used in various biomedical applications. Such materials are highly photosensitive and have applications in biosensors with fluorescent materials **[3-6]** for trapping solar radiation. It is reported that the CdS NPs have also been synthesized in many other environments like non-aqueous solvents **[7]**, reverse micelles **[8, 9]** vesicles **[10]** and zeolites **[11-12]** including other dimensional and non-dimensional materials. Thus, the quantum dots of nanometer size in areas of semiconductor with superior fluorescent properties possess remarkable optical and electronic properties that can be tuned precisely by changing their size and composition **[13-14].**

Therefore, we have developed a new method in heterogeneous medium for CdS NCs synthesis by dispersion of the required amounts of $Cd^{+2}$ and $S^{-2}$ in a specified medium supporting $Cd^{+2} + S^{-2} = CdS$, Cadmium Sulphide Encounters (CSE). The CSE is noted method for synthesizing and developing the CdS in the form of NCs. Since CdS NCs have both refractive and reflective modes of the optical light. Therefore, it could be further modified with $TiO_2$ and ZnO for nanothin films. The applications of optical, electronic and Nano photonics for the CdS NCs with most interesting physicochemical properties of FD, the CdS NCs have been boost up the optical abs. properties of FD due to its multi-functional and multi-oscillation sites and groups, the interacts the functional groups and oscillation sites for the splitting and enhance the abs.

Several scientists have studied the synthesis methods and applications of CdS NPs, but still UV-Vis enhancement of fluorescent dyes with CdS NCs have not been covered which inspired us to choose this study. The current studies on CdS NCs could enrich their potential

and technological applications in field solar enhancement with the FD dyes for the reference of e.g. RB, SRB and CF.

## Experimental

### *Materials and methods*

### *Chemicals*

All chemicals and reagents, $CdCl_2$, FeS (AR 99.5%), conc. $H_2SO_4$ (himedia, India), the RB (99.8%), SRB and CF (99.5%) procured from Sigma Aldrich, India. The XRD, AFM, HR-TEM, XPS, have characterized and the UV-Vis spectrophotometer we assumed optical absorbance of CdS NCs with FD. The maximum solutions have been prepared with chosen above chemicals and reagents with millipore water of $3x10^{-6}$ $\mu s^{-1}cm^{-1}$.

### *CdS NCs preparation*

For the development of CdS NCs, 40 % aqueous solution of $CdCl_2$ w/v was prepared on dried hydrogen sulphide ($H_2S$) gas purged by 2.0 mB pressure at RT in the clear aqueous $CdCl_2$ solution, after passing of the $H_2S$ gas the solvent changed into a dark yellow (fluorescent) colloidal solution. Separately the $H_2S$ gas was prepared from the following chemical reaction.

$$H_2SO_4+FeS \longrightarrow FeSO_4+H_2S$$

The CdS NCs were prepared on increasing the solubility product of CdS as below:

$$CdCl_2+H_2S \longrightarrow CdS+2HCl$$

The process was completed ~ 45 min to convert $CdCl_2$ clear solution to a yellow colloidal form on a continuous stirring @ 350 rpm up to 48 hrs. by using a magnetic stirrer. The colloidal solution was kept under the uninterruptedly for ~ 45 min, after saturation of the CdS NCs filtered through whatman filter paper size 42. The residue was washed 15 times with chilled water, after that collected and dried in vacuum oven for 48 hr. at 70ºC, the resultant fluorescent yellow crystal materials was noted as CdS NCs. It was subjected for physical structural characterization using several spectroscopy and hi-tech-Instruments. Thus, a whole procedure applied in our work is proposed as CSE method. After a complete structural characterization, the 100 µM CdS NCs were dispersed with 100 µM Fluorescent Dyes (FD) like RB, SRB and CF separately in water, methanol and ethanol for UV-Vis measurement.

## Results and discussion

XRD patterns were analysed on a Diffractometer D8 advanced model of Bruker with Cu Kα irradiation where the λ=1.54 nm. Consequently, CdS NCs have pure cubic, hexagonal structures and their size was calculated with the Debye Sheerer [38] equation as given below:

$$Db = \frac{K\lambda}{\beta \cos 2\theta}$$

where, Db defines the size of crystalline domain, equal to grain size, Kα dimensionless shape factor, λ from X-ray wave length, $\beta$ line bordering at FWHM and θ is Bragg angle. The 6.5, 6.5, 6.8, 6.5, 6.5, 7.0 and 6.7 nm sizes of respected miller indices show 100, 80, 60, 48, 24, 12 and 2% abundance are the intensity respectively (**Table 1**).

**Table 1**. The 6.5, 6.5, 6.8, 6.5, 6.5, 7.0 and 6.7 nm sizes of respected miller indices show 100, 80, 60, 48, 24, 12 and 2% abundance are the intensity respectively.

| D (size of crystalline domain Å ) | Angle 2θ | I (Intensity) % | h | k | l | Size of NPs (nm) |
|---|---|---|---|---|---|---|
| 3.56 | 24.993 | 80 | 1 | 0 | 0 | 6.5 |
| 3.35 | 26.587 | 48 | 0 | 0 | 2 | 6.6 |
| 3.14 | 28.401 | 100 | 1 | 0 | 1 | 6.5 |
| 2.45 | 36.650 | 24 | 1 | 0 | 2 | 6.7 |
| 2.07 | 43.694 | 60 | 1 | 1 | 0 | 6.8 |
| 1.90 | 47,835 | 48 | 1 | 0 | 3 | 6.9 |
| 1.76 | 51.911 | 44 | 1 | 1 | 2 | 7.0 |
| 1.72 | 53.211 | 12 | 2 | 0 | 1 | 7.1 |
| 1.58 | 58.357 | 2 | 2 | 0 | 2 | 7.2 |
| 1.40 | 66.763 | 15 | 2 | 0 | 3 | 7.6 |
| 1.35 | 69.583 | 3 | 2 | 1 | 0 | 7.7 |
| 1.33 | 70.785 | 7 | 2 | 1 | 1 | 7.8 |
| 1.30 | 72.675 | 3 | 1 | 1 | 4 | 7.8 |
| 1.25 | 76.084 | 15 | 2 | 1 | 2 | 8.0 |
| 1.19 | 80.678 | 5 | 2 | 1 | 2 | 8.3 |
| 1.16 | 83.219 | 14 | 2 | 1 | 3 | 8.5 |
| 1.12 | 86.907 | 5 | 0 | 0 | 6 | 8.7 |
| 1.07 | 92.094 | 3 | 1 | 0 | 6 | 7.7 |
| 1.03 | 96.811 | 2 | 2 | 2 | 0 | 6.5 |

HR-TEM model no. JEOL JEM 2100F, a highly accurate and effective instrument had determined the sizes, poly crystallinity and position of NCs with interspacing distance. Elemental estimation made by HR-TEM with JEOL JEM 2100F based on Energy Dispersive X-ray (EDAX) showed the Cd and S elements respectively. Due to the inability of CdS NCs to record the phase of an electron wave, the amplitude and image plane recorded the cluster depicted in **Fig. 1 (a)** and uniform batch of a selected and expanded area of the diameter of NCs with 7.0 nm. Therefore, separate locations of crystals have been measured in **Fig. 1 (b)** 4.92, 6.184, 7.501, 7.846 and 8.978 nm with an average size of 7.08 nm. The individual crystals tracked and subjected for diffraction by a condenser aperture on the focusing beam at cross over section screen

The surface examined by AFM, Park System model no. XE-70 at RT as well as non-contact mode with Si cantilevers of a 1650 type with a nominal tip radius of 10 nm and ≈ 220 kHz resonant frequencies. The AFM technique has investigated the surface topography of NCs. The topographic features being visible on different length allowed the moving of an identical scan area after the CdS NCs dispersion. The AFM images were recorded within

 

5µm diameter at a specimen region on glass slides. The different particles measured at high resolution and the average crystal found 7.0 nm size and the height was 2.49 nm. The AFM has been also supported to XRD and HR-TEM size too.

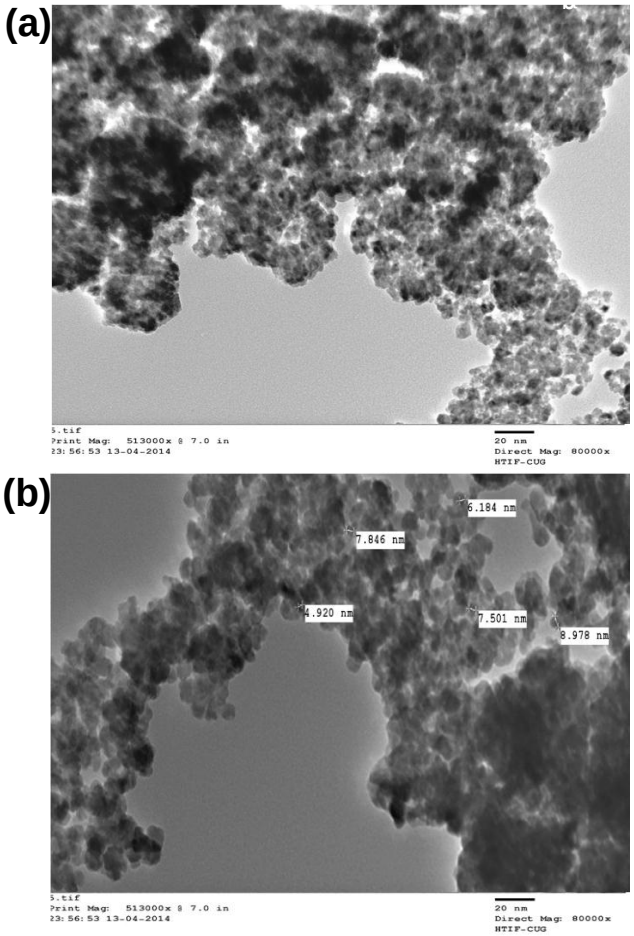


**Fig. 1.** (a) Area selected for the crystal size measurement of the CdS NCs by HR-TEM, (b) High magnification image with identified crystal size of selected CdS NCs and the average size is 7.08nm.

**Fig. 2** shows the surface topography image of CdS NCs. As shown in **Fig. 2 (a and b)** surface morphology, size and height **(c)** represents the 3D topography with their height and histogram of the CdS NCs. The height information from AFM images can be used as an exact particle diameter due to spherical NCs. The (**Fig. 2a)** size measurements by the AFM, as well as XRD **(Table-1)** and HR-TEM (**Fig. 1a)**. An average NCs diameter was considered as a mean of the largest and smallest dimensions at perpendicular diameter. **(Fig. 2a)** infers AFM TGI with diameter of 7.0 nm size.

X-ray photoelectron spectroscopy (XPS) measurements have been made with the Omicron nanotechnology unit Electron Spectroscopy for Chemical Analysis (ESCA) with Ultra High Vacuum (UHV) having Al Kα photon energy 1486.6 eV at 5.4 x $10^{-9}$ mB vacuum of analysis chamber. The multichannel detectors have been applied for detecting of photoelectron and spherical analyser 300 Watts voltage used for X-ray flux of the spectrometer was calibrated. The binding energy differs with ± 0.2 eV with literature values **[15]**. Electron impulse is in Counts per Second (CPS) of innermost electrons of solid salts **[16]** and CdS. The XPS spectra were acquired at eV energy, 2 mm slit width and take off angle of 35° with a large number of channeltron detection limits have been increased.

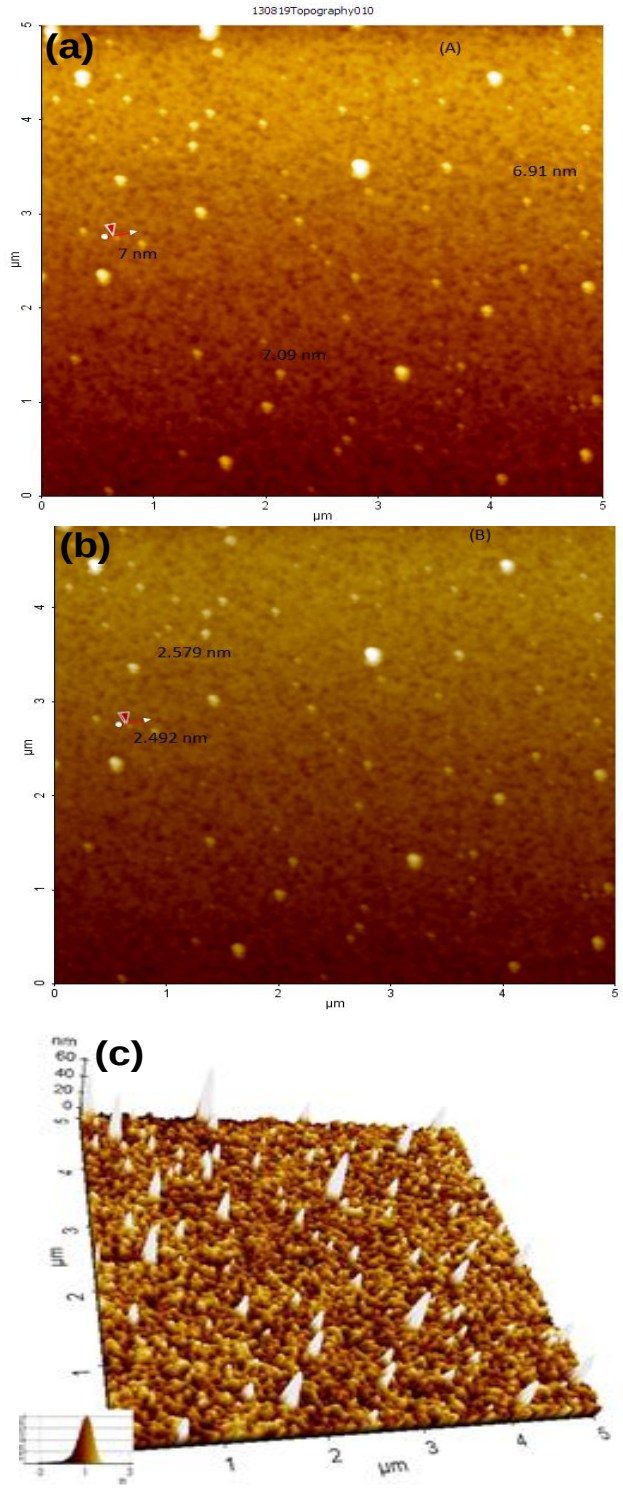


**Fig. 2.** (a) AFM topographical image for crystal size measured in different scan areas, average size is 7.0 nm (b) AFM topographical image for height measurement, the average height is 2.49 nm (c) 3D topographical image of CdS NCs.

 

The 1.6 eV FWHM resolution was found for Cd 1.0960 levels **[17]**. **Fig. 3 (a)** displays a full scan of binding energy (BE) levels of CdS NCs. The Cd 3d and S 2p core levels of CdS NCs, with a full scan of kinetic energy (KE) levels. The Cd 3d spectrum in each case has a double features due to spin orbit splitting resolution into $3d_{5/2}$ and $3d_{3/2}$ peaks with spin orbit separation by 6.7 eV. The $3d_{5/2}$ and $3d_{3/2}$ peaks of CdS have FWHM 1.0723 eV and the peak positions are at 405.93 and 412.67 eV respectively. The Cd 3d core levels fitted with a single spin orbital pair at 405.93 Cd $3d_{5/2}$ and 412.63 Cd $3d_{3/2}$. **Fig. 2 (b)** represents KE of Cd $3d_{5/2}$ and $3d_{3/2}$ samples have the 1074.50 and 1080.76 eV. The S 2p spectrum in each due to spin orbit splitting resolution into $2p_{1/2}$ and $2p_{3/2}$ 163.5 eV and the KE of S $2p_{1/2}$ and $2p_{3/2}$ 1324.36 and 1323.17 eV respectably.

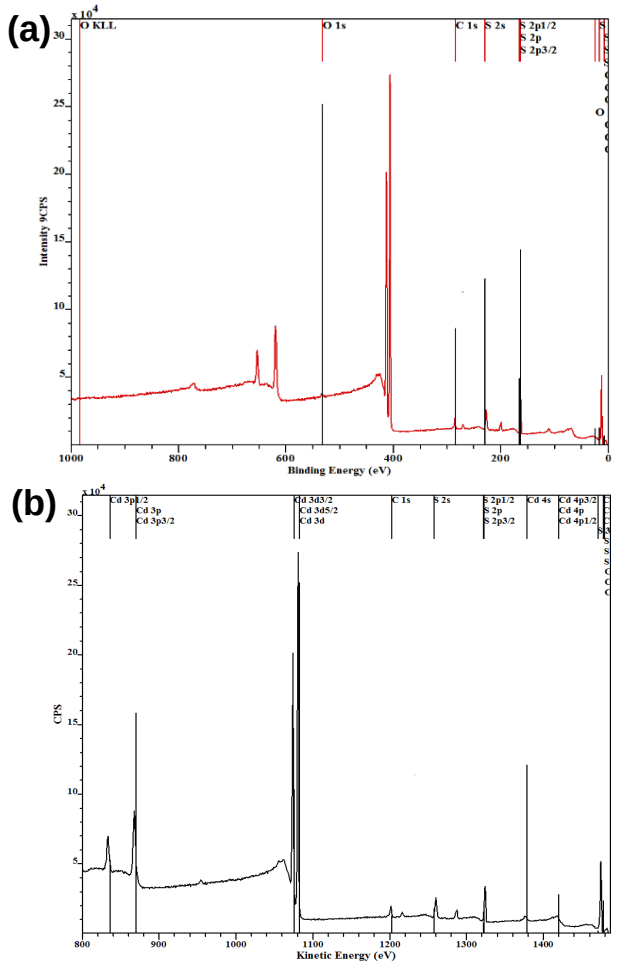


**Fig. 3.** (a) Binding and (b) kinetic energies of CdS NCs for identifying of the 3d and 2p orbital of cadmium and sulphur element respectively.

The abs. values with RB and SRB both are much closed to each other in a range of 200-320 nm. Ethanol and water show a similar splitting pattern which further intensified within 220-260 nm and rests of the zones are as usual. However, the CdS with methanol at 260 nm, the longer $\lambda_{max}$ at lower energy is obtained. The interaction of CdS NCs with fluorescent dyes depicted with UV-Vis spectrophotometer, graphical abstract **Fig**. The aqueous RB and SRB with CdS NCs showed a significant splitting at 4.0 and 3.8 abs. from 200-300 nm respectively, due to π- π-π conjugation in dyes that causes a minor splitting from 325-375 nm. The major and minor values of $\lambda_{max}$ are as RB + W = 2.9, RB + W + CdS = 4.0, SRB + W = 3.0, SRB + W + CdS = 3.8, CF + W = 3.7, CF + W + CdS = 4.0 (**Fig**. graphical abstract). Abs. of RB+W, RB+W+CdS, SRB+W, SRB+W+CdS, CF+W and CF+W+CdS mixture. However, for aqueous CdS NCs there is no splitting in the UV spectra from 200 to 320 nm as compared to dyes π conjugation. Thus, in light of above the methanol finds abs.. as RB + M = 3.2, RB + M + CdS = 4.0, SRB + M = 3.1, SRB + M + CdS = 3.1, CF + M = 3.2, CF + M + CdS = 3.1 (**Fig 1**). The CdS dispersed in methanol with the dyes, gave prominent splitting in abs. at 4.0 within 200–320 nm may be due to the activity of the π conjugation. However, the dyes without CdS had produced no significant splitting. In case of ethanol the abs. has found as RB + E = 2.8, RB + E + CdS = 3.3 SRB + E = 2.9, SRB + E + CdS = 3.3. CF + E =3.0, CF + E + CdS = 3.1 (graphical abstract **Fig**.). Similarly the CdS with dyes in ethanol caused a prominent splitting with 3.3 abs. attributed to the π conjugation of dyes, but without CdS it showed a slight splitting at the 2.8 abs. at 200-320 nm. The above mentioned difference in splitting pattern with the CdS had inferred a role of the CdS in inducing an additional ability of the dyes for higher UV light absorption. The interaction study of CdS NCs with RB, SRB and CF had caused a major splitting for CdS NCs which induced π conjugation with water and ethanol but the methanol denotes hypochromic change. It infers that the methanol has no effective response on CdS NCs with dye. For example, the interaction of CF dye with CdS in aqueous represents extra-splitting 4.0 from 220-250 nm. However the methanol and ethanol didn't show any significant shifting in the case of the CF dye with CdS NCs. A mild splitting had confirmed a weaker interaction of dye with CdS NCs in VU region. Since the whole dye molecules might be under reorientation, rotation and vibration with 10π conjugation bonds with RB, SRB and CF which induce a minor splitting on rotational motion. Due to 4 ethylene, 1-O, 1-COOH the RB oscillate behaving as functional molecule therefore the SRB having the 2 additional sulphide and the CF doesn't having any ethylene and sulphide group. When the blanked dyes are subjected to UV-vis then they undergo no tailoring interactions with CdS which found a role of the lone pair electrons causing a maximum splitting. Probably the RB seems to involve in the complex form with CdS, due to the nature of Cd, a heavy metal that does not favour the vibrational energy. The tertiary and quaternary N of the RB and SRB dyes, does not show optical abs. at 500-600 nm with ethylene group and remaining $SO_3H$ and COOH groups showed high splitting due to the more vibrations with CdS NCs. Due to an absence of quaternary and tertiary N groups from CF dye does not exist optical abs. in 450 to 600 nm range. The spectra show more splitting causes more oscillation of functional groups with the CdS NCs. While the molecules show very less splitting by the

 

second part of oscillation or vibration due to particular UV range. Meanwhile the 4 ethyl and 10π conjugations groups of RB having a maximum of 45%, however SRB having to the same, but due to the presence of sulphide groups represents less and however due to the presence of Intra Hydrogen Bonding (IHB) with sulphur that played an important role for abs. The CF neither having the ethyl group and nor IHB so the CF shows a very less abs. (**graphical abstract Fig**.)

## Conclusion

We synthesized CdS NCs and functionalized them with (RB, SRB, and CF) for the optical study and also found that the optical density of dyes increases by adding CdS NCs. The binding and kinetic energies show the strong binding of the Cd and sulphur molecules. The size confirmed with XRD, AFM and HRTEM as well as crystal structure and miller indices by the powder X-ray diffraction. After the lots of characterizations, the optical density shows that the CdS NCs increases the abs. as a nanosensor. Moreover, CdS NCs synthesis in aqueous solution has defined a nature of nanocrystals, the long term stability of the CdS NCs. Further, it could be used as nanosensor for drug carrier in pharmaceutical industries for determination of properties in pigments and targeted drug delivery, molecular imaging, and diagnosing the infected cells and tissue. The all applications are able to functioned due to its below 8.0nm size.

### Acknowledgements

We are thankful to Prof. Man Singh, our supervisor and Dean, School of Chemical Sciences/Centre for Nanosciences and Central University of Gujarat for Central Infrastructural facilities (CIF) for this research work.

### References

1. Klein, S.; Zolk, O.; Fromm, M.F.; et al; *Biochemical and Biophysical Research Communications*, **2009**, *387*, 164. **DOI:** 10.1016/j.bbrc.2009.06.144
2. Li D.; Yan Z. Y.; Cheng W. Q.; *Spectrochimica Acta Part A*, **2008**, *71*, 1211. **DOI:** 10.1016/j.saa.2008.03.024
3. Kamruzzaman K.M.; Selim; Kang I. K.; *Macromolecular research*, **2009**, *17*, 6, 410. **DOI:** 10.1007/BF03218881
4. Jiang S.; Kumara M.; Gnanasammandhan; *et al*; *J. R. Soc. Interface*, **2010**, *7*, 18. **DOI:** 10.1098/rsif.2009.0243
5. Medintz I.L.; Uyeda H. T.; Goldman E. R.; *et al; Nat. Mater*, **2005**, *4*, 446. **DOI:** 10.1038/nmat1390
6. Chan W. C. W.; Maxwell D. J.; Gao X.; *et al; S. Curr. Opin. Biotechnol*, **2002**, *13*, 46. **PMID:** 11849956
7. Eastoe J.; Hollamby M. J.; Hudson L.; *Advances in Colloid and Interface Science*, **2006**, *128*, 15. **DOI:** 10.1016/j.cis.2006.11.009
8. Liu Z.; Zhang J.; Gao B.; *Chem. Commun*., **2009**, 6918 **DOI:** 10.1039/b914588e
9. Liu Y.; Li Y.; He J.; *et al; J. Am. Chem. Soc.*, **2014**, *136*, 2610. **DOI:** 10.1039/C4PY00100A
10. Grancaric M.; Tarbuk A.; Kovacek I.; *Chemical Industry & Chemical Engineering Quarterly*, **2009**, *15*, 210. **DOI:** 10.2298/CICEQ0904203G
11. Shameli K.; Ahmad M. B.; *International Journal of Nanomedicine*, ***2011***, *6*, 331. **DOI:** 10.2147.IJN.S17112
12. Inwati G.K.; Rao Y.; Singh M.; *Nanoscale Res Lett.*, **2016**, *11*, 458. **DOI:** 10.1186/s11671-016-1653-9
13. Chun W. J.; Ishikawa A.; Fujisawa H.; *et al; J. Phys. Chem. B*, **2003**, *107*, 1803. **DOI:** 10.1021/jp027593f
14. Schneider, G.; Decher, G.; *Langmuir*, **2008**, 24: 1778–1789. **DOI:** 10.1021/la7021837
15. Rao Y.; Inwati G.; Kumar A.; *et al; International Journal of Current Engineering and Technology*, **2014**, 4, 2492. **E-ISSN:** 2277–4106, P-ISSN 2347-5161
16. Cullity B.D.; Stock S.R.; Elements of X-Ray Diffraction, 3rd Ed., Prentice-Hall Inc., **2001**, 171. **ISBN:** 0-201-61091-4
17. A.K. Singh (ed.), "Advanced X-ray Techniques in Research and Industries", Ios Pr Inc, **2005**. **ISBN:** 1586035371
18. Alexei V.; Richardson T.; *Langmuir*, **1997**, *13*, 12. **DOI:** 10.1021/la962115f

 